Surface morphology and properties of *Bombyx mori* silk fibroin fiber treated with I_2-KI aqueous solution

Md. Majibur Rahman Khan, Yasuo Gotoh [*] , Hideaki Morikawa, and Mikihiko Miura
Faculty of Textile Science and Technology, Shinshu University, Tokida 3-15-1, Ueda, Nagano 386-8567, Japan
[*] *Corresponding author. Tel: +81-268-21-5366, Fax: +81-268-21-5454.*
E-mail address: ygotohy@shinshu-u.ac.jp

ABSTRACT

The surface morphology, thermal and mechanical properties of *Bombyx mori* silk fibroin (SF) fiber treated with a 1.23 N iodine-potassium iodide (I_2-KI) aqueous solution were investigated using scanning electron microscopy (SEM), atomic force microscopy (AFM), differential scanning calorimetry (DSC), thermogravimetric (TG) analysis, and tensile measurements to clarify the effects of the iodine treatment. SEM and AFM analyses indicated that the SF fiber surface became rougher by the absorption of polyiodide ions. The mechanical properties of iodinated SF showed an increase in Young's modulus, and strain remained constant although ultimate tensile strength slightly decreased. The thermal stability of SF molecules was greatly enhanced by iodine treatment. Iodinated SF fibers should be an attractive candidate for biomedical applications such as for producing antimicrobial filters, iodine containing wound-healing anion exchange fibers, etc.

Keywords: Silk fibroin, Iodine treatment, Surface morphology, Mechanical properties, Thermal characteristics.

INTRODUCTION

Silk fiber, produced by *Bombyx mori (B. mori)* larva, is a remarkable biological protein polymer, and has been used as a textile grade fiber and surgical suture for thousands of years because of its unique textile properties such as fineness, gloss, handle, mechanical properties etc. The study of its structures, chemical, physical and mechanical properties have been extensively reviewed by various authors [1-3].

Silk typically consists of two different proteins, fibroin and sericin. Fibroin is the structural protein of silk fiber, whereas sericin is the water soluble proteinaceous glue that serves to bond the fibers together. The majority of fibroin's composition is highly periodic, with simple repeating sections broken by more complex regions containing amino acids with bulkier side chains. The highly repetitive sections are composed of glycine (45%), alanine (30%), and serine (12%) in a roughly 3:2:1 ratio and dominated by $[Gly\text{-}Ala\text{-}Gly\text{-}Ala\text{-}Gly\text{-}Ser]_n$ sequences. Fibroin is known to form mainly three kinds of conformations: silk I with a helical conformation, silk II with an antiparallel β-sheet, and a random coil without definite orders. Sericin, which comprises approximately 25wt% of the silkworm cocoon, contains glycine, serine, and aspartic acid totaling over 60% of the overall composition [4-5].

In recent years, interest in silk fibroin (SF) has been rapidly increasing because of the

advent of new applications, particularly in biomedical fields, such as scaffolds for tissue engineering [6], drug delivery systems [7], artificial skin, [8], cartilage tissue [9], biosensors [10], artificial bone regeneration [11], and wire ropes for the substitution of the anterior cruciate ligaments [12] etc. This interest arises from the unique mechanical properties of SF [13,14] and its excellent biocompatibility, environmental stability, biodegradability and the capacity to support cell and tissue growth [15,16]. For diversification of silk products, physical and chemical treatment, polymer-alloying or blending with other polymers are important techniques to improve inferior properties.

Iodine is an essential trace element for human and animals. Iodine and its derivatives find principal uses in pharmaceutical and medical applications, sanitation or disinfectants, animal feed, catalysts, inks, colorants, photographic equipment, and stabilizers. Among many modification techniques for polymers, iodine treatment has antibacterial activity. Owing to its greatest commercial importance, many iodinated products are being been developed in biomedical field, such as, iodinated cadexomer, a polysaccharide including iodine, is applied to a pharmaceutical material as a wound healing medicine, due to its high antibacterial activity [17], antiseptic wipes containing PVP iodine and glycerol [18], insulin amyloid fibrils form an inclusion complex with mol iodine: a misfolded protein as a nanoscale scaffold [19], iodine containing wound-healing anion exchange fiber [20], and rollers containing iodine compounds for disinfections [21], etc. Iodine also used to develop many filters, such as, filter for air cleaning from radioactive iodine [22], antimicrobial filters and their use for masks [23], and iodine releasing absorbent pad for rendering hazardous liquids inert [24].

Aiming to develop new products from iodinated SF, several researchers reported on iodine treatment of SF fiber [25-29]. The appearance of a new X-ray interference has been reported in the meridional reflection following introduction of iodine into SF of *Bombyx mori* type, which indicates the possibility of structural change in crystalline regions [25]. The iodination of silk and the iodine-absorption power of SF have been investigated [26]. In our previous report [29], we explained the iodine sorption behavior, structural conformation, and viscoelastic behavior of iodinated SF. We proposed a mesophase model to elucidate the new sharp reflection on the meridional direction, corresponding to a period of 7.0 Å of iodinated SF fiber. However, until recently, the surface characteristics, thermal and mechanical properties of iodinated SF have not been studied yet.

In this study, we reported the surface morphology, thermal and mechanical properties of iodinated SF fiber using scanning electron microscopy (SEM), atomic force microscopy (AFM), differential scanning calorimetry (DSC), thermogravimetric (TG) analysis, and tensile testing.

MATERIALS AND METHODS

Materials

B. mori raw silk fiber, kindly provided by the 'Dainippon Silk Foundation' Japan, was first degummed to remove sericin. The degumming process was performed by standard marseille soap / soda ash method [29,30]. In the degumming method, a weight loss of about 23.5wt% occurred indicating removal of all or most of the sericin. The degummed samples were soft and smooth to handle with a fine sheen.

Iodine Treatment

At first, a 1.23 N iodine-potassium iodide (I_2-KI) aqueous solution was prepared in a tube and kept about 24 h at room temperature with gentle stirring to dissolve iodine into potassium iodide properly. The degummed *B. mori* SF fibers were wound on a teflon plate (80mm length) to constrain fiber length and immersed in the 1.23 N I_2-KI aqueous solution for one week (168 h) at laboratory atmosphere, 25 °C and 65% relative humidity (RH). After immersion, the fiber was sufficiently rinsed with distilled water and dried in an electric oven at 95 °C for 3 h.

Sample preparation

We used 10 individual lots of degummed SF fibers for the experiments. Each lot was divided into two sub portions. In each lot, one portion was observed as original specimen and another portion was treated with 1.23 N I_2-KI aqueous solutions. Finally, untreated and iodinated specimens of 10 individual lots were used for different experiments.

Measurements

SEM Analysis

The morphologies of the fibers were examined with a Hitachi S-2380N SEM at 15 kV of acceleration voltage. Before placing the samples in the SEM chamber, the samples were mounted onto an aluminum stud and sputter- coated with gold/palladium for 180 s (E-1010 ION SPUTTER, Hitachi, Japan) to prevent charging. 10 tests were carried out (from 10 individual lots) to study SEM images.

AFM Analysis

AFM was developed as an instrument mainly used for surface science research. AFM is frequently applied to polymer surfaces, primarily to reveal the surface morphology, nanostructure, chain packing, and chemical conformation. It also provides information on nanometer-scale features, which cannot be obtained by other microscopic techniques [31]. An SPI3800N system (Seiko Instruments Inc.) with an SPA-400 multi-function type scanning probe microscopy was used for the AFM measurement. The measurements were performed using contact modes. The dimensions of the scanned areas were 2 µm × 2 µm. The scanning line frequencies were 0.5 Hz. All the scanned images were obtained using a 20 µm scanner. For contact-mode images, we used an SN-AF01 cantilever and a tip (Si_3N_4, triangular base, 100 µm long) with a radius of 20

μm. Its natural resonance frequency was 40 kHz and spring constant was 0.09 N/m. The average roughness results were obtained from 10 individual tests (from 10 individual lots).

Thermal Properties

DSC measurement was carried out with a Rigaku ThermoPlus DSC 8230 at a scanning rate of 10 °C min^{-1} in an N_2 atmosphere. 10 tests (from 10 individual lots) were carried out.

TG analysis was performed with a Rigaku ThermoPlus II 8120 at a scanning rate of 10 °C min^{-1} in an N_2 atmosphere. 10 tests (from 10 individual lots) were performed.

Mechanical Properties

The tensile properties were measured with a Tensilon Model RTC 1250A, (Orientec Corporation), Japan using standard technique at 22 °C and 65%RH at a gauge length of 40 mm and strain rate of 100% min^{-1}. 20 individual measurements (from each of 10 individual lots) were performed.

RESULTS AND DISCUSSIONS

Surface Morphology

SEM was used to analyze the change of the surface morphology of the untreated and iodinated SF fibers. SEM observation revealed a very smooth surface of the untreated SF fibers [Figure 1(a)]. These results consistent with previous cited SEM results of degummed SF fibers [32]. After iodine treatment, the fibers show a progressive change of the surface morphology. The fiber surface became rough, and some spots appeared on the fiber surface [Figure 1(b)]. The changes occurring on the fiber surfaces may be due to the cross-linking effects of iodine molecules into SF. To further investigate the surface morphology of iodinated SF, AFM analysis has been carried out.

Figure 2 illustrates the AFM images of untreated and iodinated SF fibers. It is observed that the surface topography of the SF fibers changed qualitatively after iodine treatment. The surface of untreated SF was comparatively smoother. After iodine treatment, the fiber surfaces became notably uneven, many concavo-convex surfaces were observed, and the depth and number of pits increased. Moreover, many irregular condensation clusters appeared on the SF surface. Table 1 shows the values of the surface roughness of untreated and iodinated SF fiber obtained by AFM analysis. The data were obtained from the measurements of the 2 μm × 2 μm AFM images. The average roughness (R_a) is defined as the average of the absolute values of the difference between the standard level and the selected level. It is defined as JIS B0601 and expressed by the following formula.

$$R_a = (1/S_0)\int_{Y_B}^{Y_T}\int_{X_L}^{X_R} |F(X,Y) - Z_0| dXdY \qquad (1)$$

where $F(X,Y)$ is the field which all measurement data shows; S_0 is the area when the selected level is assumed to be ideally flat; Z_0 is the average of the values of Z within the selected level. The root mean square roughness (R_{rms}) is the square root of the average of the square of the deviation from the standard level to the selected level. R_a and R_{rms} increased after iodine treatment. It is observed that iodine treatment causes the

generation of concavo-convex states, pits, clusters, and cavity on the surface and consequently increases the surface roughness.

Thermal Behavior

The thermal behavior of iodinated SF fiber was investigated by means of DSC measurement. The DSC curve [Figure 3(a)] exhibited two broad endotherms, one at low temperature (58 °C), due to loss of moisture, another at high temperature (endo peak at 310 °C), attributed to thermal decomposition of SF fiber with oriented β configuration [33]. The typical endotherm patterns of SF were remarkably changed after iodine treatment [Figure 3(b)]. The first endo peak became boarder and shifted slightly to lower temperature from 58 °C to 54 °C. Between two major endotherms, two peaks are observed at 188 °C and 275 °C, respectively. This indicates that polyiodide ions mainly are entered into the amorphous regions of SF fiber, and weaken the hydrogen bonding between amide groups. As a result, molecular chains in amorphous state are relaxed, consequently the orientation of the crystallites is decreased. At the same time, the relaxed molecular chains of the amorphous regions can move more easily, and a part of them transform to the mesophase structure. By analyzing the structural features of iodinated SF by XRD and FT-IR, we previously proposed a mesophase model of the microstructure of iodinated SF [29]. The DSC trace of iodinated SF strongly supports the formation of mesophase structure. It should be noted that the prominent endothermic peak of thermal decomposition of iodinated SF was shifted to slightly higher temperature from 310 °C to 317 °C with respect to that of the untreated one. The slightly higher decomposition temperature can be related to the presence of intermolecular cross-linking of SF with polyiodide ions such as I_3^- and I_5^-. To further investigate the thermal characteristics of iodinated SF, TG measurements were performed.

A thermogravimetric analysis is very useful to determine quantitatively the degradation behavior and the composition of the fiber. Figure 4 shows TG curves for both the untreated and iodinated SF fibers. For the untreated SF fiber, the initial weight loss below 100 °C is attributed to the evaporation of water, and is followed by nearly constant weight from 80 to 270 °C. A second large weight loss takes place in the temperature range from 270 to 400 °C. This is associated with the degradation of side chain groups of amino acid residues and the cleavage of peptide bonds [34]. After iodine treatment, the onset temperature of the second weight loss was shifted to approximately 220 °C. This may be related to not only degradation of SF, but also vaporization of the iodine component in the sample, because ca. 20wt% of polyiodide ions are included in the sample [29], and evaporation of most of the iodine component was confirmed during the TG measurement. Above 400 °C, the TG curve trend for each sample was almost coincident. Since the initial weight of the iodinated SF sample contains an iodine component of 20wt%, it can be said that the final residual carbon weight would be higher than that of the untreated one. This may be related to the intermolecular cross-linking of SF by iodination, which may cause inhibition of volatile component containing carbon from SF during heating and lead to higher carbon yield.

Mechanical Properties

The evaluation of the tensile properties is vital for producing new products from iodinated SF fibers and applications in textile and non-textiles field. Figure 5 shows the stress-strain curves of untreated and iodinated SF and the results of the tensile measurements are summarized in Table 2. The tensile strength of iodinated SF fibers was a little lower compared with that of the untreated SF. Tensile strength loss may be due to the intermolecular cross-linking of SF with polyiodide ions, which causes the hydrolysis of some sensitive peptide bonds. The strain almost remained constant, the Young's modulus increased after iodine treatment. Iodinated SF fibers had lower average orientation than that of untreated SF, the polyiodide ions enter chiefly into the amorphous region of SF fibers, which disturbed the arrangement of the fibroin chains in the non crystalline regions and partially hindered their mobility when subjected to tension, and causes to increase rigidity of the fibers.

CONCLUSIONS

To elucidate the effects of iodine treatment on SF, the fiber was treated with a 1.23 N iodine-potassium iodide (I_2-KI) aqueous solution, and the surface morphology, thermal and mechanical properties of iodinated SF fiber were investigated with SEM, AFM, DSC, TG analysis, and tensile measurements. SEM and AFM analyses indicated that the fiber surface became rougher after iodine treatment. The iodine treatment causes the generation of concavo-convex states, pits, and clusters on the surface and consequently increases the surface roughness. The thermal stability of SF molecules was greatly enhanced by iodine treatment. The mechanical properties of iodinated SF showed an increase in Young's modulus, and strain remained constant although ultimate tensile strength slightly decreased.

ACKNOWLEDGMENTS

This study was supported by a Grant-in-Aid for the Global COE Program by the Ministry of Education, Culture, Sports, Science and Technology of Japan.

Literature Cited

1. Marsh, R.E., Corey, R.B., Pauling, L., An investigation of the structure of silk fibroin, *Biochim. Biophys. Acta*. **16(1)**, 1 –34 (1955).
2. Jiang, P., Liu, H., Wang, C., Wu, L., Huang, J., Guo, C., Tensile behavior and morphology of different degummed silkworm (*Bombyx mori*) cocoon silk fibers, *Mater. Lett.*, **60**, 919 –925 (2006).
3. Lucas, F., Shaw, J.T.B., Smith, S.G., In: Anfinsen, C.B., Anson, M.L., Bailey, K., John, T., editors. Advances in Protein Chemistry, vol. 13. New York: Academic Press, pp. 107-242 (1958).
4. Zhang, H., Magoshi, J., Becker, M., Chen, J.Y., Matsunaga, R., Thermal properties of *Bombyx mori* silk fibers, *J. Appl. Polym. Sci.* **86**, 1817-1820 (2002).
5. Kaplan, D.L., Mello, C.M., Arcidiacono, S., Fossey, S., Senecal, K., Muller, W., In: McGrath, K., Kaplan, D., Editors. Protein Based Materials, Birkhauser: Boston, Chapter 4 (1997).
6. Min, B.M., Jeong, L., Nam, Y.S., Kim, J.M., Kim, J.Y., Park, W.H., Formation of silk fibroin matrices with different texture and its cellular response to normal human keratinocytes, *Int. J. Biol. Macromol.* **34**, 223-230 (2004).
7. Tsukada, M., Freddi, G., Minoura, M., Allara, G., Preparation and application of porous silk fibroin materials, *J. Appl. Polym. Sci.* **54**, 507-514 (1994).
8. Wang, Y.Z., Kim, H.J., Gordana, V.N., Kaplan, D.L., Stem cell-based tissue engineering with silk biomaterials, *Biomaterials* **27,** 6064-6082 (2006).
9. Darja, M., Augst, A., Freed, L.E., Vepari, C., Fajardo, R., Patel, N., Gray, M., Farley, M., Kaplan, D.L., Gordana, V.N., Bone and cartilage tissue constructs grown using human bone marrow stromal cells, silk scaffolds and rotating bioreactors, *Biomaterials* **27,** 6138-6149, (2006).
10. Furuhata K, Deno S, Sakamoto M., Immobilization of alkaline phosphatase onto aminated silk fabrics, *J. Seric. Sci. Jpn.* **66**, 11-16 (1997).
11. Tamada Y, Furuzono T, Taguchi T, Kishida A, Akashi M., Ca-adsorption and apatite deposition on silk fabrics modified with phosphate polymer chains, *J. Biomater. Sci. Polym. Ed.* **10(7)**, 787-794 (1999).
12. Altman, G.H., Horan, R.L., Lu, H.H., Moreau, J., Martin, I., Richmond, J.C., Kaplan, D.L., Silk matrix for tissue engineered anterior cruciate ligaments, *Biomaterials* **23**, 4131-4141 (2002).
13. Shao, Z., Vollrath, F., Surprising strength of silkworm silk, *Nature* **418**, 741 (2002).
14. Khan, M.M.R., Morikawa, H., Gotoh, Y., Miura, M., Ming, Z., Sato, Y., Iwasa, M., Structural characteristics and properties of *Bombyx mori* silk fiber obtained by different artificial forcibly silking speeds, *Int. J. Biol. Macromol.* **42(3)**, 264-270, (2008).
15. Meinel, L., Hofmann, S., Karageorgiou, V., Kirker-Head, C., McCool, J., Gronowicz, G., Zichner, L., Langer, R., Novakovic, G.V., Kaplan, D.L., The inflammatory responses to silk films in vitro and in vivo, *Biomaterials* **26**, 147–155 (2005).
16. Altman, G.H., Diaz, F., Jakuba, C., Calabro, T., Horan, R.L., Chen, J., Lu, H.,

Richmond, J., Kaplan, D.L., Silk-based biomaterials, *Biomaterials* **24,** 401–416 (2003).
17. Dixon, David, M., Wound care dressing comprising saccharide fibers, USA Patent application 2006062834, 20 pp., (2006).
18. Kelly, Albert, R., Saferstein, L., Antiseptic wipes containing PVP iodine and glycerol, USA Patent application 2006246120, 6 pp., (2006).
19. Dzwolak, W., Insulin amyloid fibrils form an inclusion complex with mol. iodine: a misfolded protein as a nanoscale scaffold, *Biochemistry*, **46(6)**, 1568-1572 (2007).
20. Ampegelova, N.I., Ivanov, V.D., Kornienko, V.N., Kritskii, V.G., Krupennikova, V.I., Rybkin, N.I., Filter for air cleaning from radioactive iodine. Russian Patent application 2262758, 8 pp., (2005).
21. Sozaki, M., Antimicrobial filters and their use for face masks, *Jpn. Kokai. Tokkyo. Koho.* 2005028230, 5 pp., (2005).
22. Beloborodov, V.L., Krylov, V.E., Saifullin, T.A., Iodine containing wound-healing anion exchange fiber. Russian Patent application 2238760, (2004).
23. Code, Kenneth R., Iodine releasing absorbent pad for rendering hazardous liquids inert. Can. Pat. Appl. 2278959, 16 pp., (2001).
24. Oyanagi, M., Rollers containing iodine compounds for disinfection, *Jpn. Kokai. Tokkyo. Koho.* 2004113729, 6 pp., (2004).
25. Friedrich-Freksa, H., Kratky, O., Sekora, A., Occurrence of new x-ray interferences by introduction of iodine into silk fibroin of the Bombyx mori type, *Naturwissenschaften*, **32**, 78 (1944).
26. Raymond, M., Rosalind, R. Pitt., The iodination of silk fibroin, *Biochimica. Et. Biophysica. Acta.*, **2**, 223-225 (1948).
27. Takahashi, T., Studies on natural silk. I. Iodine-absorbing power of silk fibroin, *J. Soc. Chem. Ind.(Japan)*, **31**, 152-155 (1928).
28. Huebner, J., Sinha, J.N., The action of iodine upon cellulose, silk and wool, *J. Soc. Chem. Ind.(London)*, **41**, 93-94 (1922).
29. Khan, M. M. R., Gotoh, Y., Miura, M., Morikawa, H., Nagura, M., Influence of iodine treatment on the structure and physical properties of *Bombyx mori* silk fibroin., *J. Polym. Sci. Part-B: Polym. Phys.*, **44**, 3418-3426 (2006).
30. Kato, H., Silk Processing Techniques and Its Application; Elsevier; Amsterdam, Chapter 1, pp. 18–19 (1968).
31. Gould, S.A.C., Shulman, J.B., Schiraldi, D.A., Occelli, M.L., Atomic force microscopy (AFM) studies of liquid crystalline polymer (LCP) surfaces. *J. Appl. Polym. Sci.*, **74**, 2243–2254 (1999).
32. Arai, T., Freddi, G., Innocenti, R., Tsukada, M., Biodegradation of Bombyx mori Silk Fibroin Fibers and Films, *J. Appl. Polym. Sci.*, **91**, 2383-2390 (2004).
33. Magoshi, J., Nakamura, S., Studies on physical properties and structure of silk. Glass transition and crystallization of silk fibroin, *J. Appl. Polym. Sci.* **19,** 1013–1015 (1975).
34. Freddi, G., Tsukada, M., Beretta, S., Structure and physical properties of silk fibroin/polyacrylamide blend films, *J. Appl. Polym. Sci.*, **71**, 1563-1571 (1999).

LIST OF TABLES AND FIGURES

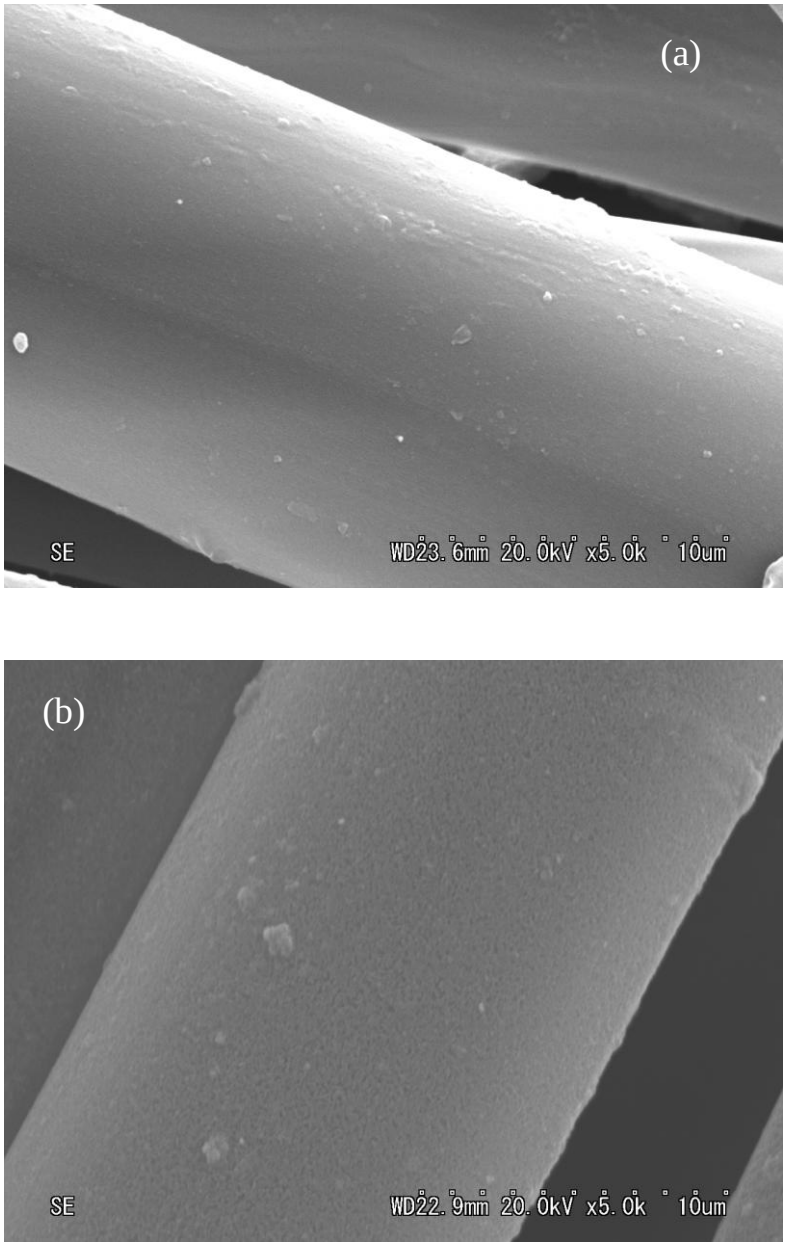

FIGURE 1. SEM images of SF fiber treated with 1.23 N I_2-KI aqueous solution for 168 h; (a) untreated SF, (b) iodinated SF.

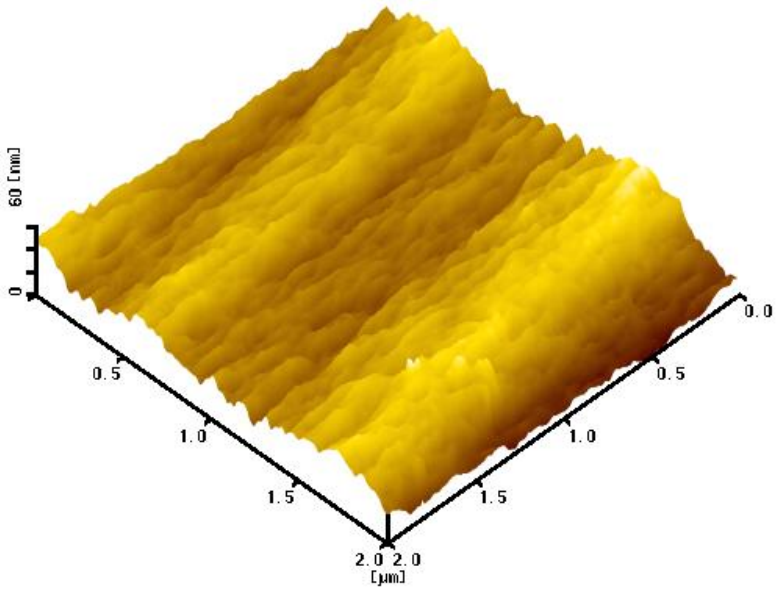

(a)

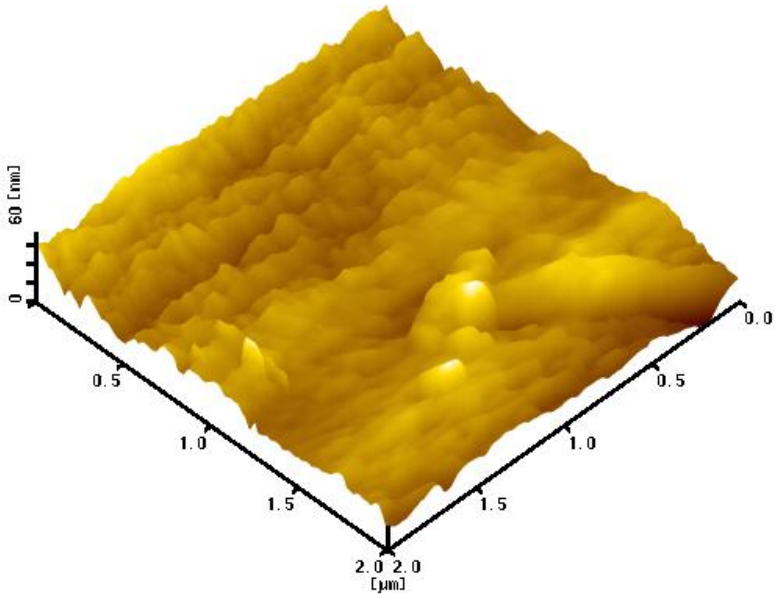

(b)

FIGURE 2. 3D AFM topographic images of SF fiber treated with 1.23 N I_2-KI aqueous solution for 168 h; (a) untreated SF, (b) iodinated SF.

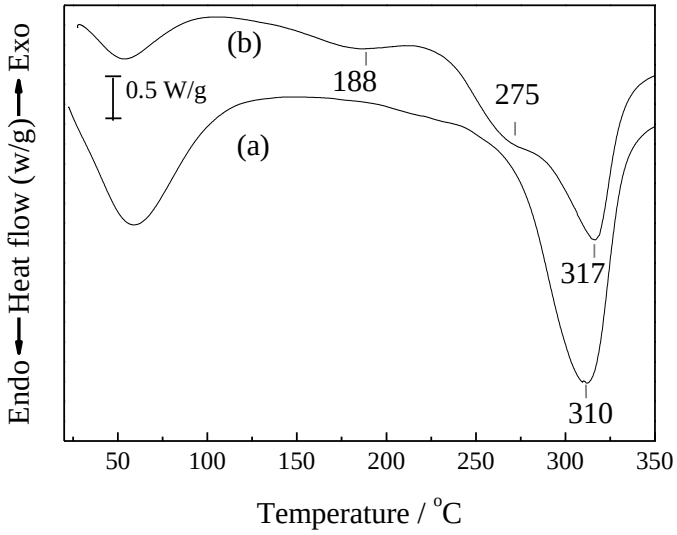

FIGURE 3. DSC thermograms of SF fiber treated with 1.23 N I_2-KI solution for 168 h; (a) untreated SF, (b) iodinated SF.

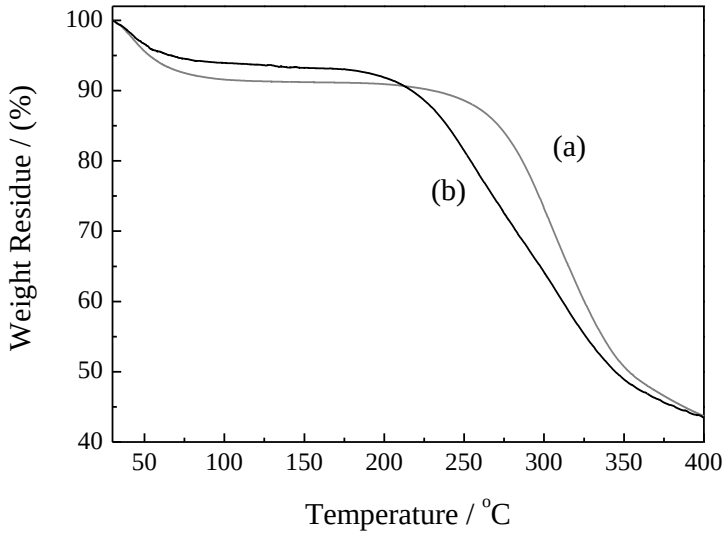

FIGURE 4. TG curves for SF fiber treated with 1.23 N I_2-KI solution for 168 h; (a) untreated SF, (b) iodinated SF.

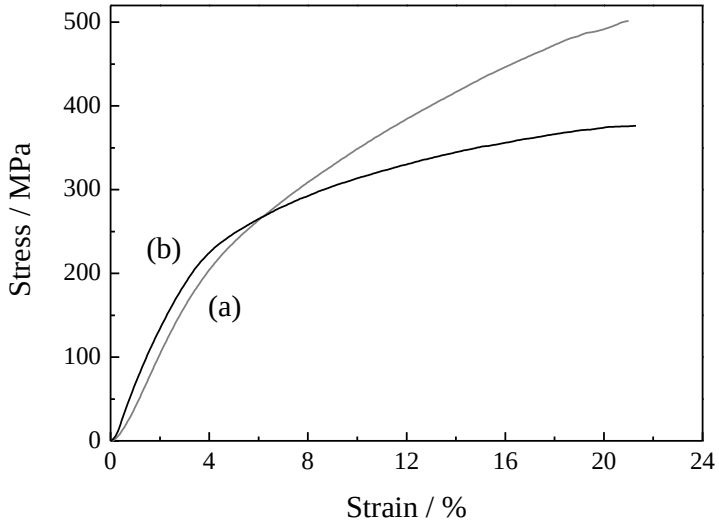

FIGURE 5. Stress-strain profiles of SF fiber treated with 1.23 N I_2-KI solution for 168 h; (a) untreated SF, (b) iodinated SF.

TABLE 1 Surface roughness values of SF fiber treated with 1.23 N I_2-KI solution for 168 h, determined from AFM analysis.

Sample	Average roughness (nm)	RMS roughness (nm)	Surface volume (nm^3)
Untreated SF	8.098	9.902	4.21E+06
Iodinated SF	9.139	12.210	4.58E+06

TABLE 2 Statistical data of mechanical properties of SF fiber treated with 1.23 N I_2-KI solution for 168 h.

Specimen	Property	Mean value	Maximum value	Minimum value	Standard deviation	Standard error
Untreated SF	Young's modulus (GPa)	6.4	6.8	5.6	0.34	0.07
	Ultimate tensile strength (GPa)	0.498	0.518	0.486	0.011	0.002
	Strain (%)	22.6	24.0	21.2	0.93	0.21
Iodinated SF	Young's modulus (GPa)	7.4	8.0	7.0	0.30	0.06
	Ultimate tensile strength (GPa)	0.384	0.401	0.372	0.011	0.002
	Strain (%)	21.9	23.5	19.5	1.20	0.26